

SEISMIC PROTECTION OF CABLE-STAYED BRIDGES UNDER MULTIPLE-SUPPORT EXCITATIONS

Shehata E. ABDEL RAHEEM¹, Toshiro HAYASHIKAWA²

ABSTRACT

For the structural control of seismic-induced vibrations of long-span cable-supported bridges, it is extremely important to include the effects of the ground motion spatial variation in the analysis and design of effective control systems. Since, the spatial variation of the ground motion plays an important role in the structural response, as has been shown in recent earthquakes. So, the control system should be designed not only to mitigate the dynamic component of the structural response but also to counteract the effects of the pseudo-static component of the response. The feasibility and efficiency of passive and active control strategies for the vibration control of cable-stayed bridge under multiple support excitations have been examined to enhance a structure's ability to withstand dynamic loading. Comparison of the response due to non-uniform input ground motion with different wave propagation velocities with the response due to uniform input demonstrates the importance of accounting for spatial variability of excitations. The control systems are shown to perform well when earthquake motions are uniform at all supports along the entire cable-stayed bridge, however, under multiple-support excitations, the performance of the control system with these parameters get worse dramatically over almost all of the evaluation criteria. The assumption of uniform earthquake motion along the entire bridge may be unrealistic for long span bridges since the differences in ground motion among different supports due to travelling seismic waves could result in quantitative and qualitative differences in seismic response. Design codes and retrofitting techniques must be upgraded to take into account the spatial variation of the seismic input.

Keywords: Cable-stayed bridges, Seismic protection, Seismic response control, Spatial ground motion

INTRODUCTION

Long span cable-stayed bridges represent aesthetically appealing lifeline structures, the increasing popularity of these bridges can be attributed to the full and efficient utilization of structural materials, increased stiffness over suspension bridges, efficient and fast mode of construction, and relatively small size of substructure (Ali and Abdel-Ghaffar, 1995; Abdel Raheem and Hayashikawa, 2003). However, from the structural dynamics point of view, long span cable-stayed bridges exhibit flexible and complex behavior in which the vertical, lateral, and torsional motions are often strongly coupled that raises many concerns about their behavior under environmental dynamic loads such as wind and earthquakes (Ganev *et al.*, 1998; Fujino, 2002); the spatial variation of the ground displacements and accelerations plays an important role in the determination of the structural response (Lin *et al.*, 2004), as has been shown in recent earthquakes (Loma Prieta 1989, Northridge 1994, Hyogo-Ken Nanbu 1995). So, it is extremely important to include the effects of the spatial variation of the ground motion in the analysis, design and tuning of mechanical systems for the vibration control of seismic induced vibrations of long-span cable-supported bridges. In this way, the control system should be designed not only to mitigate the dynamic component of the structural response but also to counteract the effects of the pseudo-static component of the response.

¹ JSPS Fellow, Graduate School of Engineering, Hokkaido University, Japan, Email: shehata@eng.hokudai.ac.jp

² Professor, Graduate School of Engineering, Hokkaido University, Japan, Email: toshiroh@eng.hokudai.ac.jp.

The focus of this study is to use the benchmark bridge model of Dyke *et al.* (2000) to investigate the feasibility and efficiency of different control strategies for seismic protection of cable-stayed bridges under multiple support excitations. The effect of spatial variations of ground motion with different wave propagation apparent velocities on the performance of seismic control systems for cable-stayed bridges is studied to enhance a structure's ability to withstand dynamic loading, earthquake excitation of a bridge on multiple supports is derived and the prospects for active and passive control of the bridge motion are explored. Passive systems do not require an external power source and respond to the local motion of the structure. These systems offer the ability to dissipate the vibratory energy in the structure, reducing the number of cycles that the structure will experience (Soong, 1990; Iemura and Pradono, 2002; Abdel Raheem and Hayashikawa, 2003). Semi-active systems generate a control force based on measurements of the structure's responses at designated points, hence can adapt to a wide range operating conditions and structures. The application of semi-active control system to civil engineering structures is very promising [Jansen and Dyke, 2000; Caicedo *et al.*, 2003; Abdel Raheem and Dorka, 2006; Abdel Raheem *et al.*, 2007]. Control forces are developed based on feedback from sensors that measure the excitation and/or the response of the structure, the feedback of the response may be measured at locations remote from the active control system. With the HYsteretic DEvice Systems; HYDES (Dorka *et al.*, 1998) being independent of the vertical load bearing system, a wide variety of link hysteresis loops are possible for optimal performance, a complete control over the maximum forces is possible in the main horizontal load resisting system regardless of the type and severity of the earthquake. To effectively implement control systems on structural systems it is necessary to know which type of control system will achieve better performance on the structure under consideration. This will lead to the development of guidelines for selecting the most appropriate control system for a structure. A systematic comparison of the performance of passive and active systems in reducing the structure's responses is performed.

The effect of the spatial variability of the ground motion in the analysis of seismically controlled long span bridges is considered based on the decomposition of the total structural response into a dynamic component and a pseudo-static component. Comparison of the response due to non-uniform input with the response due to uniform input demonstrates the importance of accounting for spatial variability of excitations, different wave propagation velocities are undertaken in the dynamic analysis of the controlled cable-stayed bridge. The control systems are shown to perform well when earthquake motions are uniform at all supports along the entire cable-stayed bridge, however, under multiple-support excitations, the performance of the control system with these parameters get worse dramatically over almost all of the evaluation criteria. Moreover, bridges subjected to spatially variable input motions are characterized by excitation of higher modes which are primarily anti-symmetric. The assumption of uniform earthquake motion along the entire bridge, however, may be unrealistic for long span bridges since the differences in ground motion among different supports due to travelling seismic waves may result in quantitative and qualitative differences in seismic response as compared with those produced by uniform motion at all supports. Design codes and retrofitting techniques must be upgraded to take into account the spatial character of the seismic input.

BRIDGE FINITE ELEMENT MODEL FORMULATION

This study considers the cable-stayed bridge shown in Figure 1, which is located in Cape Girardeau, Missouri, USA. Based on detailed drawings of the bridge, a three-dimensional finite element model has been developed by Dyke *et al.* (2000) to represent the complex behavior of the full-scale benchmark bridge shown in Figure 2. The linear evaluation model was developed and used as a basis of comparison of the performances using various protective systems. Three earthquake records, each scaled to peak ground accelerations of 0.36g or smaller, used for numerical simulations are: (i) El Centro NS (1940); (ii) Mexico City (1985); and (iii) Gebze N-S (1999). Evaluation criteria J_1 to J_{18} have been established in (Dyke *et al.*, 2000); however, only the evaluation criteria J_1 to J_{13} are relevant to semi-active and passive systems and hence used in the present study, these evaluation criteria have been normalized by the corresponding response quantities for the uncontrolled bridge.

Equation of Motion of Controlled Bridge Subjected to Multiple Seismic Excitations

Considering the general equation of motion for a cable-stayed bridge subjected to uniform seismic loads, the dynamic equation of motion can be written as

$$\mathbf{M}\ddot{\mathbf{U}} + \mathbf{C}\dot{\mathbf{U}} + \mathbf{K}\mathbf{U} = -\mathbf{M}\Gamma\ddot{\mathbf{x}}_g + \Lambda\mathbf{f} \quad (1)$$

where \mathbf{U} is the displacement response vector, \mathbf{M} , \mathbf{C} and \mathbf{K} are the mass, damping and stiffness matrices of the structure, \mathbf{f} is the vector of control force inputs, $\ddot{\mathbf{x}}_g$ is the longitudinal ground acceleration, Γ is a vector of zeros and ones relating the ground acceleration to the bridge degrees of freedom (DOF), and Λ is a vector relating the force produced by the control device to the bridge DOFs. This is appropriate when the excitation is uniformly applied at all supports of the structure. For the analysis of the bridge with multiple-support excitation, the model must include the supports degrees of freedom. The equation of dynamic equilibrium for all the DOFs is written in partitioned form (Caicedo *et al.*, 2003)

$$\begin{bmatrix} \mathbf{M} & \mathbf{M}_g \\ \mathbf{M}_g^T & \mathbf{M}_{gg} \end{bmatrix} \begin{bmatrix} \ddot{\mathbf{U}}^t \\ \ddot{\mathbf{U}}_g \end{bmatrix} + \begin{bmatrix} \mathbf{C} & \mathbf{C}_g \\ \mathbf{C}_g^T & \mathbf{C}_{gg} \end{bmatrix} \begin{bmatrix} \dot{\mathbf{U}}^t \\ \dot{\mathbf{U}}_g \end{bmatrix} + \begin{bmatrix} \mathbf{K} & \mathbf{K}_g \\ \mathbf{K}_g^T & \mathbf{K}_{gg} \end{bmatrix} \begin{bmatrix} \mathbf{U}^t \\ \mathbf{U}_g \end{bmatrix} = \begin{bmatrix} \mathbf{0} \\ \mathbf{P}_g \end{bmatrix} + \begin{bmatrix} \Lambda\mathbf{f} \\ \mathbf{0} \end{bmatrix} \quad (2)$$

Where \mathbf{U}^t and \mathbf{U}_g are the superstructure absolute displacement vector and the supports enforced ground displacement vector, respectively; \mathbf{M}_g , \mathbf{C}_g and \mathbf{K}_g are the mass, damping and elastic-coupling matrices expressing the forces developed in the active DOFs by the motion of the supports. \mathbf{M}_{gg} , \mathbf{C}_{gg} and \mathbf{K}_{gg} are the mass, damping and stiffness matrices of the supports, respectively. It is desired to determine the displacement vector \mathbf{U}^t in the superstructure DOFs and the support forces \mathbf{P}_g . Since the control forces \mathbf{f} are only applied to the active superstructure DOFs. The total displacement \mathbf{U}^t is expressed as its displacement \mathbf{U}^s due to static application of the ground motion, plus the dynamic displacement \mathbf{U} relative to the quasi-static displacement.

$$\mathbf{U}^t = \mathbf{U}^s + \mathbf{U} \quad (3)$$

$$\mathbf{K}\mathbf{U}^s + \mathbf{K}_g\mathbf{U}_g = \mathbf{0} \quad (4)$$

In which, \mathbf{U}^s is the pseudo-static displacement vector. In the model, the seismic movement of the bridge supports excites the superstructure of the bridge through the influence matrix. Solving for these displacements leads to define the pseudo-static influence vector as follow

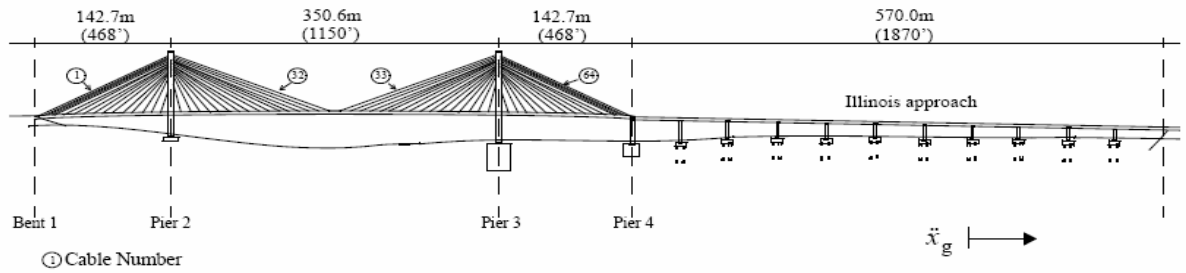


Figure 1. View of the Cape Girardeau bridge

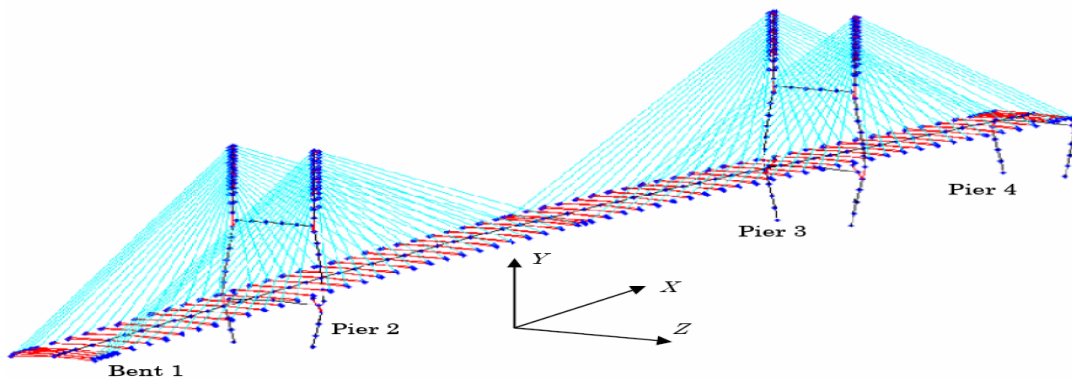


Figure 2. Bridge finite element model

$$\mathbf{R}_s = -\mathbf{K}^{-1}\mathbf{K}_g \quad (5)$$

Finally; substituting Eqs. (3), (4) and Eq. (5) into the first row of (2) gives

$$\mathbf{M}\ddot{\mathbf{U}} + \mathbf{C}\dot{\mathbf{U}} + \mathbf{K}\mathbf{U} = \mathbf{A}\mathbf{f} - (\mathbf{M}\mathbf{R}_s + \mathbf{M}_g)\ddot{\mathbf{U}}_g - (\mathbf{C}\mathbf{R}_s + \mathbf{C}_g)\dot{\mathbf{U}}_g \quad (6)$$

If the ground accelerations $\ddot{\mathbf{U}}_g$ and velocities $\dot{\mathbf{U}}_g$ are prescribed at each bridge support, this completes the governing equation formulation. The excitations are in fact non-uniform for different foundations, in this analysis; the non-uniformity of the ground accelerations is realized by using the same seismic waves but with time delays.

Bridge Benchmark Evaluation Model

The model resulting from the finite element formulation, which is modeled by beam elements, cable elements, and rigid links as shown in Figure 2, has a large number of degrees-of freedom and high frequency dynamics. Thus, some assumptions are made regarding the behavior of the bridge to make the model more manageable for dynamic simulation while retaining the fundamental behavior of the bridge. Application of static condensation reduction scheme to the full model of the bridge resulted in a 419 DOF reduced order model, the first 100 natural frequencies of the reduced model (up to 3.5 Hz) were compared and are in good agreement with those of the 909 DOF structure. The damping matrix is defined based on modal damping assumption and developed by assigning 3% of critical damping to each mode, and this value is selected to be consistent with assumptions made during the bridge design. The reduced system is used to construct the damping matrix using

$$\mathbf{C} = \mathbf{M} \Phi \begin{bmatrix} 2\zeta_1 \omega_1 & 0 & 0 \\ 0 & \dots & 0 \\ 0 & 0 & 2\zeta_n \omega_n \end{bmatrix} \Phi^{-1} \quad (7)$$

where Φ is the modal matrix, and ω_i and ζ_i are the natural frequency [rad/sec] and modal damping ratio of the i th mode, respectively. The evaluation model is considered to portray the actual dynamics of the bridge and will be used to evaluate various control systems. Because the evaluation model is too large for control design and implementation, a reduced-order model (i.e., design model) of the system should be developed. The design model given by Dyke *et al.* (2000), which has 30 states, was derived from the evaluation model by forming a balanced realization of the system and condensing out the states with relatively small controllability and observability Grammians.

MATHEMATICAL MODELING AND CONTROL STRATEGY

For a seismically excited structure, assuming that the forces provided by the control devices are adequate to keep the response of the structure from exiting the linear region, the equations of motion can be written in the following state-space form description as follow:

$$\dot{\mathbf{x}} = \mathbf{A}\mathbf{x} + \mathbf{B}\mathbf{f} + \mathbf{E} \begin{bmatrix} \ddot{\mathbf{U}}_g^T & \dot{\mathbf{U}}_g^T \end{bmatrix}^T \quad (8)$$

$$\mathbf{y}_m = \mathbf{C}_y \mathbf{x} + \mathbf{D}_y \mathbf{f} + \mathbf{v} \quad (9)$$

$$\mathbf{z} = \mathbf{C}_z \mathbf{x} + \mathbf{D}_z \mathbf{f} \quad (10)$$

In which \mathbf{x} is the state vector, \mathbf{y}_m is the vector of measured outputs, \mathbf{z} is the regulated output vector, \mathbf{v} is the measurement noise vector. The measurements typically available for control force determination include the absolute acceleration of selected points on the structure, the displacement of each control device, and a measurement of each control force. For this initial study active, semi-active and the passive devices are modeled as ideal devices. Therefore, neither actuator dynamic nor control-structure interaction is explicitly included in the device models. A description of the approach used to model and control each of these devices is provided in the following sections.

Passive Control System

One of the most widely implemented and accepted seismic protection systems is base isolation. Seismic base isolation is a technique that mitigates the effects of an earthquake by essentially isolating the structure and its contents from potentially dangerous ground motion, especially in the frequency range where the structure is most affected. Conventional base isolation devices of Lead Rubber Bearings (LRBs) are considered to passively reduce seismic responses of the bridge in this study. These bearings offer a simple passive control method and are relatively easy and inexpensive to manufacture. The design shear force level for the yielding of lead plugs is taken to be $0.10M$, where M is the part of the deck weight carried by bearings. This assumption has been widely accepted among bearing designers (Robinson, 1982; Ali and Abdel-Ghaffar, 1995). The passive control forces applied to the structure are only dependent on the motion of the structure are function of the relative displacement and velocity across the device. The compliant Lead Rubber Bearings (LRBs) installed in the bridge deck tower/bent connection of seismically isolated bridge structures protect these structures from strong earthquakes through a reduction of stiffness and an increase in damping. The reduction of stiffness is intended to detune the structures fundamental period from the characteristic period of earthquake ground motions. Isolation bearings are designed to accommodate large displacement demands and to mobilize damping mechanisms, typically through material yielding of a lead column within the isolator, Figure 3.

Semi-Active Control System

The H2/LQG control algorithm is used for the controller design using the reduced order model of the system (Dyke *et al.*, 1996). Optimal control algorithms are based on the minimization of a performance index that depends on the system variables, while maintain a desired system state and minimize the control effort. According to classical performance criterion, the active control force f_c is found by minimizing the performance index subjected to a second order system.

Control Algorithm

A nonlinear control law is derived to maximize the energy dissipated from a vibrating structure by the frictional interface using the normal force as control input. The level of normal force required is determined using optimal controller; the LQG control problem is to devise a control law with constant gain to minimize the quadratic cost function in the form

$$f_c = -\mathbf{K} x \quad (11)$$

In the design of the controller, the disturbances to the system are taken to be identically distributed, statistically independent stationary white noise process. An infinite horizon performance index is chosen that weights the regulated output vector, z

$$J = \lim_{\tau \rightarrow \infty} \frac{1}{\tau} E \left[\int_0^{\tau} \left\{ (C_z x + D_z f)' Q (C_z x + D_z f) + f^T R f \right\} dt \right] \quad (12)$$

where \mathbf{Q} and \mathbf{R} are weighting matrices for the vectors of regulated responses and control forces, respectively. Further, the measurement noise is assumed to be identically distributed, statistically independent Gaussian white noise process, with $S_w / S_v = \gamma = 25$. \mathbf{K} is the full state feedback gain

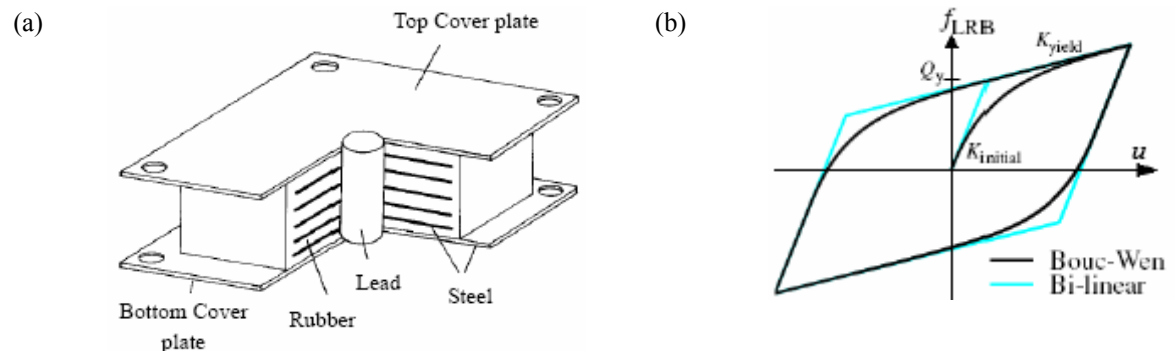


Figure 3. Passive control device: (a)LRB construction scheme, (b) Hysteretic model

matrix for the deterministic regulator problem given by

$$\mathbf{K} = \tilde{\mathbf{R}}^{-1} \mathbf{B}^T \mathbf{P} \quad (13)$$

where \mathbf{P} is the symmetric positive definite solution of the algebraic Riccati equation given by

$$\mathbf{P}\mathbf{A} + \mathbf{A}^T \mathbf{P} - \mathbf{P}\mathbf{B}\tilde{\mathbf{R}}^{-1} \mathbf{B}^T \mathbf{P} + \mathbf{C}_z^T \mathbf{Q} \mathbf{C}_z = \mathbf{0} \quad (14)$$

$$\tilde{\mathbf{R}} = \mathbf{R} + \mathbf{D}_z^T \mathbf{Q} \mathbf{D}_z \quad (15)$$

The problem with state feedback control is that every element of the state vector is used in the feedback path and, clearly, many states in realistic systems are not easily measurable. The optimal controller Eq. (11) is not implemental without the full state measurement. However, a state estimate can be formulated \hat{x} such that $f_c = -\mathbf{K} \hat{x}$ remains optimal based on the measurements. This state estimate is generated by the Kalman filter

$$\dot{\hat{x}} = \mathbf{A}\hat{x} + \mathbf{B}f + \mathbf{L}(y_m - \mathbf{C}_y \hat{x} - \mathbf{D}_y f) = (\mathbf{A} - \mathbf{L}\mathbf{C}_y)\hat{x} + \left[\mathbf{L} \mathbf{B} - \mathbf{L}\mathbf{D}_y \right] \begin{Bmatrix} y_m \\ f \end{Bmatrix} \quad (16)$$

In which \hat{x} is the Kalman filter optimal estimate of the state space vector x . \mathbf{L} is the gain matrix for state estimator with the state observer technique, determined by solving an algebraic Riccati equation, the estimator uses the known inputs f_c and the measurements y_m to generate the output and state estimates \hat{y} and \hat{x} . Kalman filter is used to estimate states of the reduced-order model required for the applications of semi-active controllers using selected acceleration and displacement measurements.

$$\mathbf{L} = \mathbf{S}\mathbf{C}_y^T \mathbf{R}^{-1} \quad (17)$$

The estimation error variance \mathbf{S} is a solution of the filter Riccati algebraic equation given by

$$\mathbf{S}\mathbf{A} + \mathbf{A}^T \mathbf{S} - \mathbf{S}\mathbf{C}_y^T \mathbf{R}^{-1} \mathbf{C}_y \mathbf{S} + \gamma \mathbf{E} \mathbf{E}^T = \mathbf{0} \quad (18)$$

Calculations to determine \mathbf{K} and \mathbf{L} are performed using the control toolbox in MATLAB. The proposed approach is to append a force feedback loop to induce the friction device to produce approximately desired control force f_c . A linear optimal controller $K_c(s)$ is then designed that provides the desired control force f_c based on the measured responses y_m , and the measured force f as Follow

$$f_c = L^{-1} \left\{ -K_c(s) L \begin{bmatrix} y_m \\ f \end{bmatrix} \right\} \quad (19)$$

where $L(\cdot)$ is the Laplace transform. Although the controller $K_c(s)$ can be obtained from a variety of synthesis methods, the H2/LQG strategies are advocated herein because of the stochastic nature of earthquake ground motions and because of their successful application in other civil engineering structural control applications. The force generated by the friction device cannot be commanded; only the voltage v applied to the current driver for the friction device can be directly changed, consequently, the air pressure could be changed. To induce the friction device to generate approximately the desired optimal control force f_c , the command signal v is selected as follows

$$v = (V_{\max} / f_{\max}) |f_c| H(\{f_c - f\}f) \quad (20)$$

where V_{\max} and f_{\max} is the device maximum voltage and force, and $H(\cdot)$ is the Heaviside step function.

Friction Device UHYDE-fbr

The friction device UHYDE-fbr dissipates energy as a result of solid sliding friction (Dorka et al., 1998; Abdel Raheem and Dorka, 2006). The patented sliding mechanism consists of two steel plates and a set of bronze inserts. One of the steel plates serves as guidance for the bronze inserts. The other plate has a specially prepared surface which is in contact with the inserts forming the sliding surface, Figure 4. The structural implementation of these devices as well as the experimental verification and evaluation of semi-active control in bridges have been experimentally investigated at the European Laboratory for Structural Assessment within the ‘‘Testing of Algorithms for Semi-Active Control of Bridges (TASCB)’’ project, financed under the ‘‘European Consortium of Laboratories for Earthquake

And Dynamic Experimental Research - JRC" (ECOLEADER) within the Fifth Framework Program of the European Commission.

Biaxial Bouc-Wen Model

In a well designed control system, the input energy due to an earthquake is largely dissipated in the control devices through friction or yielding of lead plug. The devices limit the motion of the mechanism which leads to minimized stresses in the structure. Bouc-Wen's model is used to characterize the hysteretic force-deformation characteristic of the UHYDE-fbr and LRB devices. The forces mobilized in the control device can be modeled by biaxial model as follow:

$$\begin{aligned} f_x &= c_0 \dot{u}_x + k_0 u_x + \alpha z_x \\ f_y &= c_0 \dot{u}_y + k_0 u_y + \alpha z_y \end{aligned} \quad (21)$$

where z_i is an evolutionary shape variable, internal friction state, bounded by the values ± 1 ; and account for the conditions of separation and reattachment (instead of a signum function) and the directional/biaxial interaction of device forces. The model for biaxial interaction of the resultant hysteretic forces is given as first order differential equation (Park et al., 1986):

$$\begin{bmatrix} \dot{z}_x \\ \dot{z}_y \end{bmatrix} = \begin{bmatrix} A \dot{u}_x \\ A \dot{u}_y \end{bmatrix} - \begin{bmatrix} z_x^2 (\gamma \text{sign}(z_x \dot{u}_x) + \beta) & z_x z_y (\gamma \text{sign}(z_y \dot{u}_y) + \beta) \\ z_x z_y (\gamma \text{sign}(z_x \dot{u}_x) + \beta) & z_y^2 (\gamma \text{sign}(z_y \dot{u}_y) + \beta) \end{bmatrix} \begin{bmatrix} \dot{u}_x \\ \dot{u}_y \end{bmatrix} \quad (22)$$

β , γ and A are called the characteristic parameters of the Bouc-Wen model (Park et al., 1986). β controls the nature of the constitutive law (hardening or softening). The determination of the most appropriate yielding level or slip load level at different placement locations in the structure is, thus, an important design issue which must be resolved for devices effective utilization in practice.

UHYDE-fbr Friction Device

From displacement controlled tests on the friction device under constant pressure and varying frequency, no significant dependency of the friction coefficient on the excitation frequency is observed and the average friction coefficient is determined to be 0.45. In this paper, the dynamic behavior will be neglected, so the normal force is proportional to the input voltage. In addition, the dynamics involved in the UHYDE-fbr pneumatic servo system equilibrium are accounted for through the first order filter

$$\dot{u} = -\eta(u - v) \quad (23)$$

where v is the command voltage applied to the control circuit, $\eta = 50 \text{ sec}^{-1}$ is time constant associated with filter. Analog voltage control, cover range 0 - 10 Volt is applied to air pressure regulator to set the desired analog output air pressure signal. The functional dependence of the device parameters on the command voltage u is expressed as:

$$\alpha = \alpha_a + \alpha_b u; \quad c_0 = c_{0a} + c_{0b} u \quad (24)$$

In equations (21 & 24), $\alpha = \mu N$ is function of N the clamping force and μ the coefficient of sliding friction, c_0 describes the force associated with viscous dissipation due to compressed gas. The

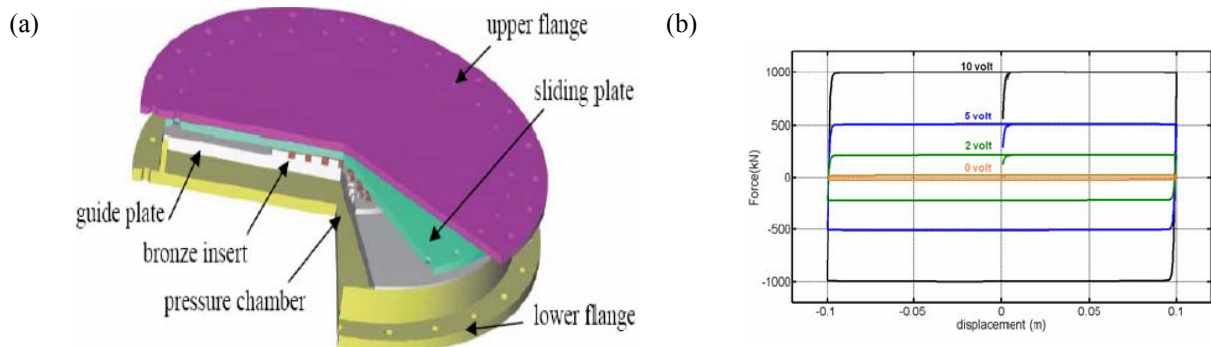


Figure 4. Semi-active control device; (a) UHYDE-fbr construction scheme (b) Hysteretic model for different input volt

parameters of the UHYDE-fbr device are selected so that the device has a capacity of 1000 kN and maximum displacement of 500 mm (the tested friction device scaled: 2.5 for the frictional force; 1.5 for displacement), as follow: $A = 1000 \text{ m}^{-1}$ and $\gamma = \beta = 500 \text{ m}^{-1}$, $c_{0a} = 10 \text{ kN.s/m}$, $c_{0b} = 25 \text{ kN.s/m.V}$, $k_0 = 25 \text{ kN/m}$, $\alpha_a = 22.5 \text{ kN}$, $\alpha_b = 101.25 \text{ kN/V}$.

Lead Rubber Bearing - LRBs

Non-linear yielding hysteretic type isolation system using LRB is studied; the nonlinear dissipative Bouc-Wen model is adopted in order to represent the dynamic behaviour of LRB isolators under a severe earthquake. The horizontal nonlinear restoring force is expressed as the sum of three forces acting in parallel given in equation (21), in which, k_0 and c_0 are the horizontal stiffness and viscous damping coefficient of the rubber composite of the bearing. $\alpha = (1 - k_0/k_e) \cdot Q_y$ is the yield force of the lead plug; Q_y is the yield force from both the lead plug and the rubber stiffness. The properties of the LRB are k_e initial elastic shear stiffness and k_0 post-yield shear stiffness, $k_0/k_e = 0.10$. To model the initial stiffness properly, it is required that $A = k_e/Q_y$. For unloading to follow the pre-yield stiffness, $A = 140 \text{ m}^{-1}$ and $\gamma = \beta = 70 \text{ m}^{-1}$, $c_0 = 100 \text{ kN.s/m}$, $k_e = 68000 \text{ kN/m}$, and $Q_y = 400 \text{ kN}$.

NUMERICAL RESULTS AND DISCUSSION

To verify the effectiveness of the presented seismic control design, simulations are done for the three historical earthquakes specified in the benchmark problem statement. Assuming that the spatially varying earthquake wave propagates in the subsoil from one end of the bridge to the other, three propagating velocities of the seismic wave in the soil 1000 and 3000m/s, as well as with infinite speed (uniform excitation) are used in the simulations. To evaluate the ability of various control systems to reduce the peak responses, the normalised responses over the entire time record, and the control requirements, evaluation criteria $J_1 - J_{13}$ that have been presented (Dyke *et al.*, 2000; Caicedo, *et. al.*, 2003) are considered. Evaluation criteria $J_1 - J_6$ are related to peak response quantities, where J_1 = the peak base shear of towers, J_2 = the peak shear force of towers at the deck level, J_3 = the peak overturning moment at the bases of towers, J_4 = the peak moment of towers at the deck level, J_5 = the peak deviation in cable tension, and J_6 = the peak displacement of the deck at the abutment. Evaluation criteria $J_7 - J_{11}$ are related to normed response quantities corresponding to response quantities for $J_1 - J_5$. Evaluation criteria $J_{12} - J_{13}$ are related to control system requirements; J_{12} = the peak control force, J_{13} = the peak device stroke.

- *Passive Control Strategy*, 24 LRBs are placed between the deck and pier/bent at eight locations in the bridge, eight between the deck and pier 2, eight between the deck and pier 3, four between the deck and bent 1, and four between the deck and pier 4. The device parameters are optimized for maximum energy dissipation and to minimize the earthquake force and displacement responses.

- *Active Control Strategy*, 24 actuators are used for sample active control described in the benchmark, while 24 friction devices are used for semi-active control through the bridge with configuration as in passive strategy. In addition to fourteen accelerometers, eight displacement transducers and eight force transducers to measure control forces applied to the structure are used for feedback to the clipped optimal control algorithm. To evaluate the ability of the friction device system to achieve the performance of a comparable fully active control system, the device is assumed to be ideal, can generate the desired dissipative forces with no delay, hence the actuator/sensor dynamics are not considered. Appropriate selection of parameters (z , Q , R) is important in the design of the control algorithm to achieve high performance controllers. The weighting coefficients of performance index are selected such that; R is selected as an identity matrix; z is comprised of different important responses for the overall behavior of the bridge that are constructed by the Kalman filter from selected measurements. Extensive simulations have been conducted to find the most effective weighting values corresponding to regulated responses, and accordingly the optimized weighting matrix Q can be selected as follows:

Semi-active control with feedback corresponding to deck displacement and tower top velocity regulated output response and weighting values as follow:

$$Q_{dd\&dv} = \begin{bmatrix} q_{dd} \mathbf{I}_{4 \times 4} & \mathbf{0} \\ \mathbf{0} & q_{dv} \end{bmatrix} \quad q_{dd} = 8092.5, q_{dv} = 4.607 \times 10^5$$

Sample active control with feedback corresponding to deck displacement and mid span acceleration regulated output response and weighting values as follow:

$$Q_{dd\&da} = \begin{bmatrix} q_{dd} \mathbf{I}_{4 \times 4} & \mathbf{0} \\ \mathbf{0} & q_{da} \end{bmatrix} \quad q_{dd} = 3222, q_{da} = 40.0$$

Simulation results of the proposed control strategies are compared for uniform and multiple excitation with two shear wave velocities of 3000 and 1000 m/s. Tables 1~3 show the evaluation criteria for all the three earthquakes, from which, it can be concluded that the different control strategies are very effective in reducing the force and displacement response, especially for ground motions with a high frequency content such as El Centro with dominant frequencies of 1.1, 1.3 and 2.1 Hz, as shown in Table 1, while the efficiency of control strategies under Mexico earthquake (dominant frequency of 0.45 Hz) and Gebze earthquake (dominant frequencies of 0.25 and 2.0 Hz) that has a lower frequency content, is decreased and resulting in a larger force and displacement responses dominated by low-order modes compared to El Centro earthquake case as shown in Tables 1~3. It is also shown the dependency of the seismic response of the controlled bridge on the frequency content of the input motion, since lower and higher order fundamental modes with frequencies close to Gebze earthquake wide range dominant frequencies are excited, resulting in higher force and displacement responses, and higher control force is required. It is observed that the different control strategies are quite effective in reducing response quantities of the bridge whenever predominant period of ground motions is close to the fundamental natural period of the bridge and less effective when the predominant periods of ground motions are far from the fundamental period of the bridge. The maximum deck displacement is less than allowable displacement (0.3 m), the tension in the stay cables remains within allowable values.

A comparative study is also performed on cable-stayed bridge benchmark equipped with passive, semi-active and active control systems with the same numbers and configurations of control devices. The passive control strategy can be designed to achieve peak response ($J_1 - J_6$) reduction comparable to the active/semi-active control strategy, while it is difficult to attain the same response reduction efficiency over the entire time history ($J_7 - J_{11}$), the member force responses can be minimized, but of course in the expense of increasing deck displacement. The passive control system creates a larger force responses reduction comparable to active controlled system, while sacrificing deck displacement of the bridge structure. To reduce the excessive displacement, higher stiffness is needed between the deck and the towers, an optimum performance with passive control system can be obtained by balancing the reduction in forces along the bridge against tolerable displacements. For the cable-stayed bridge control, it is observed that unlike the passive control system case, the proposed active and semi-

Table 1 Maximum evaluation criteria for El Centro earthquake

Criteria	Passive Control			Semi-Active Control			Sample Active Control		
	Uniform	Multiple excitation, v_s		Uniform	Multiple excitation, v_s		Uniform	Multiple excitation, v_s	
		3000 m/s	1000 m/s		3000 m/s	1000 m/s		3000 m/s	1000 m/s
J_1	0.2816	0.2867	0.3326	0.2908	0.3229	0.3329	0.2703	0.3048	0.3232
J_2	0.8258	1.0108	1.1981	0.9058	0.8532	0.8373	0.7580	0.7729	1.1105
J_3	0.3144	0.3621	0.3738	0.2339	0.2940	0.2699	0.2818	0.3452	0.3378
J_4	0.6998	0.6468	0.5699	0.4805	0.4988	0.4734	0.5713	0.5573	0.5574
J_5	0.2826	0.2235	0.3258	0.2732	0.2496	0.3013	0.2357	0.2450	0.3117
J_6	1.6461	1.6685	1.3551	1.1012	0.9890	0.6228	1.1745	1.0973	1.0155
J_7	0.2604	0.2656	0.2877	0.2336	0.2387	0.2381	0.2125	0.2225	0.2626
J_8	0.8381	0.8548	0.9530	0.8528	0.8788	0.9546	0.7872	0.8355	1.0089
J_9	0.2791	0.2904	0.2975	0.2040	0.2211	0.2066	0.2255	0.2419	0.2704
J_{10}	0.5054	0.5172	0.4790	0.5060	0.5103	0.4928	0.5960	0.6103	0.6029
J_{11}	2.56E-02	2.36E-02	3.13E-02	2.68E-02	2.49E-02	2.82E-02	2.64E-02	2.35E-02	3.16E-02
J_{12}	2.92E-03	2.95E-03	2.53E-03	1.96E-03	1.96E-03	1.96E-03	2.84E-03	2.67E-03	1.80E-03
J_{13}	1.0082	1.0220	0.8300	0.6745	0.6058	0.3815	0.7194	0.6721	0.6220

Table 2 Maximum evaluation criteria for Mexico earthquake

Criteria	Passive Control			Semi-Active Control			Sample Active Control		
	Uniform	Multiple excitation, v_s		Uniform	Multiple excitation, v_s		Uniform	Multiple excitation, v_s	
		3000 m/s	1000 m/s		3000 m/s	1000 m/s		3000 m/s	1000 m/s
J_1	0.45767	0.40360	0.3613	0.4197	0.4687	0.4964	0.3618	0.3465	0.3714
J_2	1.29301	1.16223	1.0260	1.2012	1.0637	1.2111	0.8845	0.8744	1.0270
J_3	0.62230	0.55639	0.3957	0.4156	0.3662	0.3483	0.4231	0.4046	0.3714
J_4	0.79743	0.76383	0.5692	0.6293	0.6582	0.5895	0.7430	0.7273	0.6705
J_5	0.10862	0.11912	0.1783	0.1429	0.1688	0.1687	0.1034	0.1144	0.1821
J_6	2.50670	2.36156	1.4457	1.0023	0.9963	0.9801	1.7902	1.8098	1.4890
J_7	0.39788	0.39185	0.3880	0.3501	0.3612	0.3144	0.2492	0.2637	0.2985
J_8	1.00144	1.00144	1.0223	1.0309	1.1397	1.1575	0.8331	0.8945	1.0343
J_9	0.49848	0.49226	0.4324	0.3047	0.3224	0.2594	0.2986	0.3131	0.3312
J_{10}	0.75602	0.72042	0.5224	0.5612	0.6045	0.5836	0.7502	0.7696	0.7574
J_{11}	1.65E-02	1.68E-02	2.18E-02	1.52E-02	1.61E-02	1.62E-02	1.38E-02	1.43E-02	1.76E-02
J_{12}	2.45E-03	2.35E-03	1.72E-03	1.96E-03	1.96E-03	1.96E-03	1.64E-03	1.53E-03	1.43E-03
J_{13}	1.36506	1.28602	0.7873	0.5458	0.5426	0.5337	0.9749	0.9856	0.8109

Table 3 Maximum evaluation criteria for Gebze earthquake

Criteria	Passive Control			Semi-Active Control			Sample Active Control		
	Uniform	Multiple excitation, v_s		Uniform	Multiple excitation, v_s		Uniform	Multiple excitation, v_s	
		3000 m/s	1000 m/s		3000 m/s	1000 m/s		3000 m/s	1000 m/s
J_1	0.41542	0.42732	0.4554	0.4988	0.5396	0.5431	0.4194	0.4384	0.4907
J_2	1.06076	1.03083	1.0434	1.1234	1.4687	1.0309	0.7431	0.9102	0.9563
J_3	0.47482	0.43766	0.4359	0.3552	0.4029	0.3706	0.3852	0.4156	0.4486
J_4	0.75625	0.82853	0.7864	0.6491	0.6550	0.7951	0.7916	0.8725	0.8619
J_5	0.21171	0.18872	0.2212	0.2208	0.2116	0.2221	0.1874	0.1811	0.2180
J_6	1.84583	1.84314	1.6892	1.7130	1.6967	1.4006	2.2876	2.2823	2.2259
J_7	0.41097	0.40796	0.3978	0.3270	0.3223	0.3184	0.2987	0.3043	0.3276
J_8	1.04535	1.08476	1.0852	0.9583	1.0925	1.0758	0.8603	0.9297	1.0125
J_9	0.47358	0.47179	0.4696	0.3386	0.3394	0.3504	0.3880	0.3957	0.4219
J_{10}	0.54162	0.59369	0.7018	0.6828	0.6929	0.7077	0.6988	0.7459	0.8675
J_{11}	1.88E-02	1.79E-02	2.16E-02	1.76E-02	1.65E-02	2.06E-02	1.68E-02	1.49E-02	2.07E-02
J_{12}	2.42E-03	2.42E-03	2.27E-03	1.96E-03	1.96E-03	1.96E-03	2.88E-03	2.72E-03	2.06E-03
J_{13}	0.80544	0.80426	0.7371	0.7475	0.7404	0.6132	0.9982	0.9959	0.9713

active control strategies are able to effectively and simultaneously reduce the maximum displacement and force responses. But the passive control system for this benchmark problem is a little better than the semi-active control strategy in some responses. Furthermore, multiple-support excitation can cause a significant increase in structural force responses hence, should be included in the analysis. Multiple-support excitation needs to be considered since it can excite entirely different modes than uniform-support excitation. Moreover, multiple-support excitation induces forces that are caused by pseudo-static displacements and can not be controlled. The force peak responses and normed responses over the entire record are significantly increased with the multiple excitation of low shear wave velocity, while the deck displacement response J_6 is decreased. Special attention needs to be given to coupled modes since their control can lead to an increased force response of the structure. The assumption of uniform motion along the entire bridge results in quantitative and qualitative differences in seismic response as compared with those produced by uniform motion at all supports.

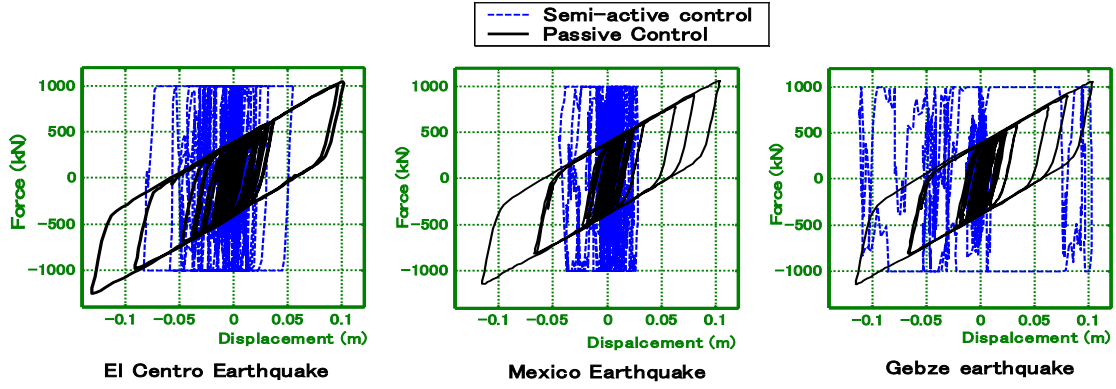


Figure 5. Hysteretic loops of control devices under uniform excitation

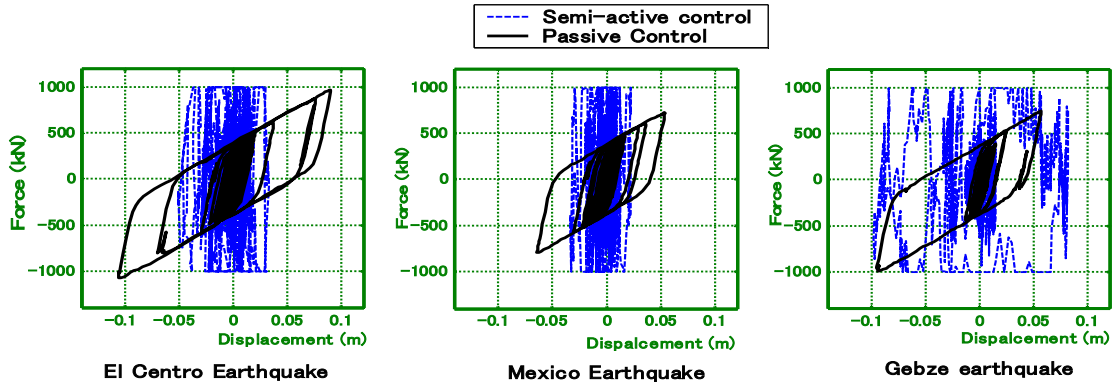


Figure 6. Hysteretic loops of control devices under non-uniform excitation ($v_s = 1000$ m/s)

Figures 5 and 6 show the hysteretic loops of control devices for passive and semi-active control strategies under uniform and non-uniform excitations, it can be observed that the efficiency of the control devices is decreased, which can be attributed to excitation of primarily anti-symmetric higher modes by spatially variable input motions that are difficult to control. The control system should be designed not only to mitigate the dynamic component of the structural response but also to counteract the effects of the pseudo-static component of the response.

CONCLUSIONS

The effectiveness of the proposed control strategies has been demonstrated and evaluated through application to the ASCE benchmark cable-stayed bridge problem subject to three historically recorded earthquakes. Three types of control devices are used to reduce the response of the deck which includes actuators for active control, UHYDE-fbr friction for semi-active control and LRBs for passive control base isolations. The modified Bouc-Wen model is considered as a dynamic model of control devices. Simulations results show that significant reduction in earthquake induced forces along the bridge can be achieved with the different control strategies as compared to the case of using conventional connections. Moreover, the different proposed control systems can significantly reduce the seismic forces transferred to the towers of the bridge with an acceptable increase in deck displacement, and simultaneously keep tensions in the stay cables within a recommended range of allowable values with very small deviation from the nominal pretension. The seismic response of the controlled bridge, hence the efficiency of the control strategy show significant dependency on the frequency content of the input motion. Unlike the passive control strategy, the proposed active and semi-active control strategies are able to effectively and simultaneously reduce the maximum displacement and force responses. The control systems are shown to perform well when earthquake motions are uniform at all supports along the entire cable-stayed bridge, however, under multiple-support excitations, the

performance of the control system with these parameters get worse dramatically over almost all of the evaluation criteria. Moreover, bridges subjected to spatially variable input motions are characterized by excitation of higher modes which are primarily anti-symmetric and difficult to control, hence reduce the efficiency of the control devices in energy dissipation. The assumption of uniform earthquake motion along the entire bridge could result in quantitative and qualitative differences in seismic response as compared with those produced by uniform motion at all supports. It is observed that the different control strategies are quite effective in reducing response quantities of the bridge whenever predominant period of ground motions is close to the fundamental natural period of the bridge and significantly less effective when the predominant periods of ground motions are far from the fundamental period of the bridge. Design codes and retrofitting techniques must be upgraded to take into account the spatial variation of the seismic input, lack of considering the traveling wave effect may lead to unsafe conclusions.

ACKNOWLEDGEMENTS

The authors gratefully acknowledge the support of this research by Japan Society for the Promotion of Science –JSPS (P06138).

REFERENCES

- Abdel Raheem, S.E. and Hayashikawa, T. "Parametric study on steel tower seismic response of cable-stayed bridges under great earthquake ground motion," *JSCCE Structural Engineering/ Earthquake Engineering*, 20(1), 25-41, 2003.
- Abdel Raheem, S.E., Dorka, U.E. and Hayashikawa, T. "Friction based semi-active control of cable-stayed bridges," *JSCCE Journal of Structural Engineering*, 53A, 2007. (Under publication)
- Abdel raheem, S.E. and Dorka, U.E "Feasibility study on semi-active control of the cable-stayed bridge benchmark with friction device system," "4th World Conference on Structural Control and Monitoring-4WCSCM , 11-13 July 2006, San Diego, California, CDROM Paper No. 32, 2006.
- Ali, H.M. and Abdel-Ghaffar, A.M. "Modeling the nonlinear seismic behavior of cable-stayed bridges with passive control bearings," *Computers & Structures*, 54(3), 461-492, 1995.
- Ali, H.M. and Abdel-Ghaffar, A.M. "Seismic passive control of cable-stayed bridges," *Shock and Vibration*, 2(4), 259-272, 1995.
- Caicedo J.M., Dyke, S.J., Moon, S.J., Bergman, L.A., Turan, G. and Hague, S. "Phase II benchmark control problem for seismic response of cable-stayed bridges," *Journal of Structural Control*, 10, 137-168, 2003.
- Dorka, U.E., Flygare, E. and Ji, A. "Passive seismic control of bridges by hysteretic device system," 2nd World Conference on Structural Control (2WCSC), Kyoto, Japan, June 27 –July 1, Proceedings, 1687–1694, 1998.
- Dyke S.J., Spencer, Jr., Sain, M.K. and Carlson, J.D. "Modeling and control of Magnetorheological dampers for seismic response reduction," *Smart Materials and Structures*, 5, 565-575, 1996.
- Dyke, S.J., Turan, G., Caicedo, J.M., Bergman, L.A. and Hague, S. "Benchmark control problem for seismic response of cable-stayed bridges," (<http://wusceel.civewustl.edu/quake/>), 2000.
- Fujino, Y. "Vibration, control and monitoring of long-span bridges-recent research, developments and practice in Japan," *Journal of Constructional Steel Research*, 58, 71-97, 2002.
- Ganev, T., Yamazaki, F., Ishizaki, H. and Kitazawa, M. "Response analysis of the Higashi-Kobe bridge and surrounding soil in the 1995 Hyogoken-Nanbu earthquake," *Earthquake Engineering and Structural Dynamics*, 27, 557-576, 1998.
- Iemura H. and Pradono, M.H. "Passive and semi-active seismic response control of a cable-stayed bridge," *Journal of Structural Control*, 9, 189-204, 2002.
- Jansen, L.M. and Dyke, S.J. "Semi-active control strategies for MR dampers: comparative study," *Journal of Engineering Mechanics*, 126(8), 795-803, 2002.
- Lin, J.H., Zhang, Y.H., Li, Q.S. and Williams, F.W. "Seismic spatial effects for long-span bridges, using the pseudo excitation method," *Engineering Structures*, 26, 1207-1216, 2004.
- Park, Y.J., Wen, Y.K. and Ang, A.H.S. "Random vibration of hysteretic system under bi-directional ground motions," *Earthquake Engineering and Structural Dynamics*, 14(4), 543-557, 1986.
- Robinson, W.H. "Lead-rubber hysteretic bearings suitable for protecting structures during earthquakes," *Earthquake Engineering and Structural Dynamics*, 10, 593-604, 1982.
- Soong, T.T. "Active Structural Control, Theory and Practice," Longman: UK, 1990.